Original Paper

Eletrônica de Potência
Open Journal of Power Electronics

Received October 16, 2025; Received in revised form January 08,2026; Accepted February 02, 2026; Date of publication March 12, 2026.
The review of this paper was arranged by Associate Editor Victor F. Mendes and Editor-in-Chief Telles B. Lazzarin
Digital Object Identifier http://doi.org/10.18618/REP.e202616

Integrated Cloud and Hardware-in-the-Loop Framework for IoT-Based Control and Monitoring

Diuary Gonçalves[1,2], Ives de O. Furtado[1], Allan F. Cupertino[1,4], Heverton A. Pereira[1,3], Remus Teodorescu[5]

[1]Centro Federal de Educação Tecnológica de Minas Gerais, Graduate Program in Electrical Engineering, Belo Horizonte, MG, Brazil.
[2]Centro Federal de Educação Tecnológica Celso Suckow da Fonseca, Department of Electrical Engineering, Nova Friburgo, Rj, Brazil.
[3]Universidade Federal de Viçosa, Department of Electrical Engineering, Viçosa, MG, Brazil.
[4]Universidade Federal de Juiz de Fora, Graduate Program in Electrical Engineering, Juiz de Fora, MG, Brazil
[5]Aalborg University, Aalborg, Denmark

e-mail: diuary.goncalves@cefet-rj.br*; ives.furtado@ufv.br ; allan.cupertino@ufjf.br ; heverton.pereira@ufv.br; ret@energy.aau.dk.
*Corresponding author.

ABSTRACT This work introduces a Cloud-in-the-Loop approach that combines Internet of Things (IoT) devices with Hardware-in-the-Loop simulation for testing control and monitoring applications. The proposed architecture employs a three-level hierarchical structure: the first level simulates the Battery Energy Storage System and local power flow control on a Digital Sampling Processor microcontroller, the second level uses an ESP32 microcontroller for Controller Area Network (CAN) communication and data transmission to the cloud, and the third level, implemented with an online broker, enables data storage, analysis and commands. A simplified power flow model and a battery model representation are considered to evaluate long-term operation with one year of climate and load data. Two load management strategies were compared: (i) total load shedding at 0% State of Charge, and (ii) hierarchical load disconnection at predefined SOC thresholds. Results showed that the hierarchical strategy increased the average State of Charge by 25.2% (54.66% vs. 43.64%), prevented interruptions to critical loads. The results show that the proposed framework serves as a flexible step before real deployment, since its cloud-based functions remain unaltered while only the physical hardware is replaced. This approach reduces implementation problems and allows the methodology to be extended to various case studies.

KEYWORDS Cloud-Based Platform, Hardware-in-the-Loop, Isolated Power Energy System, Battery Energy Storage Systems, State of Charge Management.

I. INTRODUCTION

In recent years, there has been a tendency to use Hardware-in-the-Loop (HIL) instead of conventional testing in various areas of electrical engineering. This shift is driven by factors such as cost reduction, improved safety, and increased flexibility in test setups. In many fields, this trend is evident in applications such as power electronics, electric vehicles and control systems [1]–[3].

Recent developments in testing methodologies have led to the establishment of multiple in-the-loop structures for simulation and validation in power electronics and control applications. Software-in-the-Loop (SIL) expands the Model-in-the-Loop (MIL) approach by enabling direct execution of compiled control code in software environments, supporting rapid algorithmic validation with reduced implementation effort [4]. Controller-Hardware-in-the-Loop (CHIL) further increases testing realism by deploying SIL-validated code into real or emulated embedded platforms, allowing the assessment of timing constraints, quantization effects, and digital processing limitations typical of DSP-based controllers [5]–[7]. Power-Hardware-in-the-Loop (PHIL), in turn, integrates physical hardware components into a real-time emulation framework, enabling the experimental validation of switching converters, inverter control strategies, and grid-interactive functionalities under controllable yet realistic conditions [8], [9]. Figure 1 illustrates these different in-the-loop structures, showing the progression from software-based simulations to real hardware integration and presenting the structure proposed in this work, the Cloud-in-the-Loop (CIL), which allows for Internet of Things (IoT) system testing.

Furthermore, Table 1 illustrate that each in-the-loop structure addresses distinct validation objectives [4]. While SIL and CHIL focus on control verification with low cost and flexibility, and PHIL emphasizes electrical fidelity with increased complexity, the proposed Cloud-in-the-Loop (CIL) targets system-level operational validation prioritizing realistic communication and selective continuity of critical loads.

Moreover, alongside the increased use of in-the-loop structures, another topic of interest in the literature is IoT

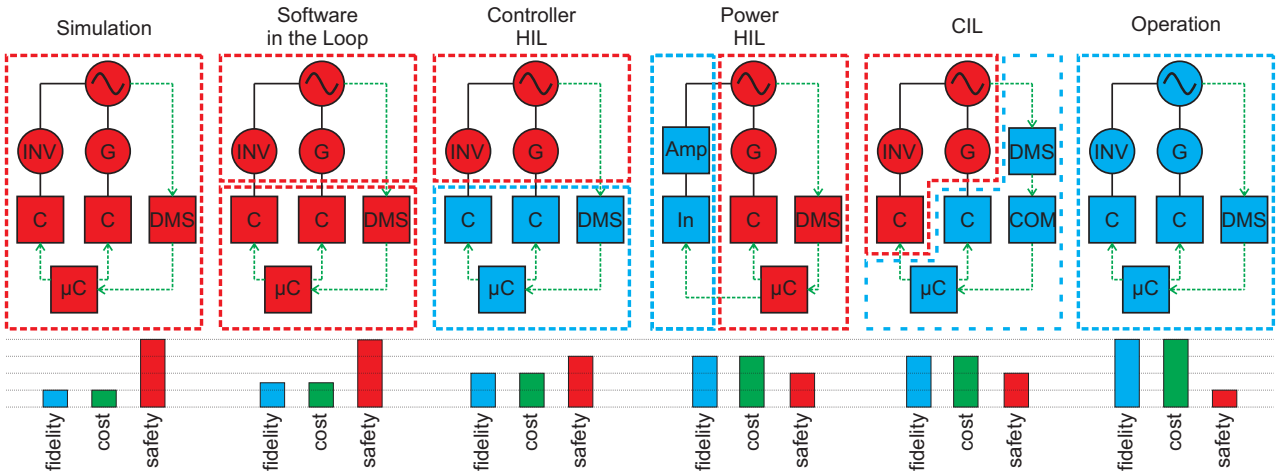

FIGURE 1. Different types of in-the-loop structures.

TABLE 1. Comparison of in-the-loop architectures

Approach	Focus	Hardware	Cost	Scal.
SIL	Control alg.	None	Very low	High
CHIL	Timing	MCU/DSP	Low	High
PHIL	Elec. fidelity	Power HW	High	Low
CIL	System oper.	Ctrl.+cloud	Moderate	High

technology, which plays a role in managing, automating, and monitoring various systems. These standalone systems can connect to the internet, enabling data transmission and reception [10]. Consequently, isolated power systems setups can forecast energy outages in remote communities by using weather forecasts, historical energy demand data, and available power reserves [11]. Recent studies in power electronics reinforce the role of IoT in energy-aware systems. One work demonstrates the use of magnetic-field energy harvesting to supply long-range IoT devices in high-current environments [12], while another highlights IoT and wireless sensing as key drivers for future advances in monitoring and automation within power electronics [13]. Additionally, through cloud data exchange and remote computing for mathematical analysis and machine learning, parameters such as battery State of Charge (SOC) and state of health can be estimated [14]. Furthermore, IoT technology is also being widely used in Industry 4.0 applications in recent years.

Considering the widespread adoption of IoT technologies in modern industrial and engineering applications, this paper proposes a new cloud-based validation architecture inspired by in-the-loop testing concepts. In the proposed framework, controller algorithms are executed on real Digital Signal Processor (DSP) hardware, while the interaction are mediated through cloud communication to emulate real-time behavior. This architecture enables a validation environment that goes beyond conventional simulation by incorporating physical control hardware and cloud connectivity, effectively bridging the gap between purely virtual validation and full hardware deployment in IoT-enabled systems. To the best of the authors' knowledge, this is the first work to jointly explore Cloud-in-the-Loop and hardware-based controller execution within this application context.

The paper is organized as follows. Section II describes the Cloud in the Loop architecture. Section III presents the power flow and energy storage models. Section IV discusses the strategy adopted to reduce load shedding. Section V details the case study and the test scenarios. Section VI presents and analyzes the results. Finally, Section VII concludes the paper and highlights its main contributions.

II. CLOUD-IN-THE-LOOP STRATEGIES

To validate the CIL structure, a combination of simulation and IoT is implemented. The simulation is carried out to compare an energy-saving strategy with total load shedding. This strategy uses a three-level hierarchical network architecture to control and monitor a Battery Energy Storage System (BESS) and loads through an IoT platform. At the first level, a simulation of the system on a local DSP microcontroller manages the power flow, representing the BESS. The second level, implemented using an ESP32, handles data management and cloud connectivity, this physical microcontroller is used for IoT communication and is connected to the DSP. The third level, supported by an online platform, in this work, the *thingable!* broker [15] is responsible for data analysis, storage, and decision-making. The hierarchical system is shown in Figure 2.

The first layer of the hierarchical control, where a BESS would be located, is simulated on the DSP, which communicates with a Controller Area Network (CAN) via a transceiver. The CAN network may incorporate multiple devices and control structures; however, their operational parameters are defined by higher-level commands, as shown in Figure 2.

The second control level can be implemented through the use of a microcontroller. This device is responsible for receiving various data packets from diverse sources of

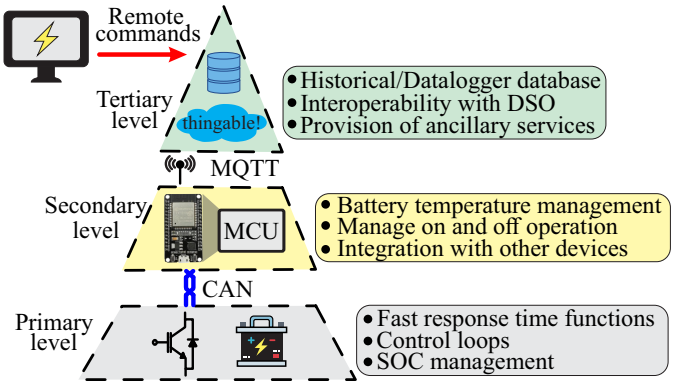

FIGURE 2. BESS hierarchical control organization.

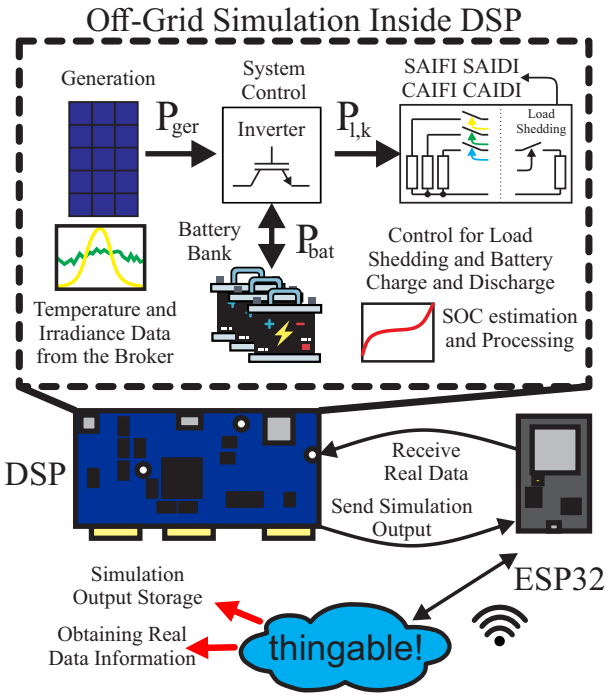

FIGURE 3. Implementation of the simulation in the DSP.

measurements within the on-site system. For instance, in the case of the BESS, it gathers information on the power system and battery currents and voltages. Additionally, it monitors battery terminal temperatures for security and operational condition assessment, with temperature data obtained through the use of Thermocouples. The microcontroller should be equipped with internet connectivity, enabling it to both send and receive commands from the broker, exchanging data with the other devices on-site through the use of CAN. All collected data on-site is transmitted to the broker for further processing.

At the third control level is the online broker, responsible for monitoring and issuing commands to the local controllers. In this implementation, the broker is deployed on a cloud-based IoT platform [15]. The platform supports: (i) real-time data storage and retrieval using a time-series database for high-frequency data logging; (ii) integration with weather APIs to obtain solar irradiance and temperature forecasts; (iii) execution of automated decision-making algorithms for load shedding with response times below 2 seconds; and (iv) historical data analysis supported by data-streaming tools such as Apache Kafka.

The broker accesses a cloud database capable of storing data from multiple devices, enabling decision-making based on both current and historical information. Communication is implemented using the MQTT protocol with QoS level 2 (exactly-once delivery), while JSON formatting is used for structured data exchange with message compression to reduce bandwidth usage. The average round-trip communication latency between the local ESP32 and the cloud platform is in the range of 150 to 300 ms, depending on internet connectivity quality.

Moreover, the system supports cloud communication via the Wi-Fi network using the MQTT protocol, allowing it to send or receive commands as needed. For example, it can retrieve weather forecasts for the upcoming days or transmit the SOC of the battery.

The purpose of the power system shown in Figure 3 is to simulate an isolated power system within a processor, specifically a DSP. The DSP is responsible for simulating the system operation, including photovoltaic power generation using irradiance and temperature profiles, the power converter integrated with the Battery Energy Storage System (BESS), and different load shedding strategies applied in each case study. Furthermore, all data required for the simulation, as well as the data produced by it, are exchanged with a cloud broker, in this case the *thingable!* platform, through an ESP32 device.

However, the model depicted in Figure 3 would be too complex to be fully implemented on a DSP if all components were explicitly modeled. Therefore, a simplified representation focused on power flow is adopted, as shown in Figure 4. In this model, the photovoltaic generation is represented by an array of PV modules reduced to an estimation of the total generated power of the photovoltaic system. The battery bank is connected to the charge controller and the inverter, both of which are modeled only through their power exchange relationships. Any excess generated power is directed to the BESS, while any power deficit is supplied by it.

The battery behavior is characterized by its State of Charge, which evolves according to the energy demanded by the system, and is modeled as a controlled voltage source with a series resistance. This simplified representation, together with the implemented load shedding strategies, allows the essential energy management dynamics of the isolated power system to be captured while ensuring real-time execution on the DSP.

The CIL approach provides several advantages over pure simulation: (i) real-time execution constraints validation, (ii) actual communication protocol testing, (iii) hardware

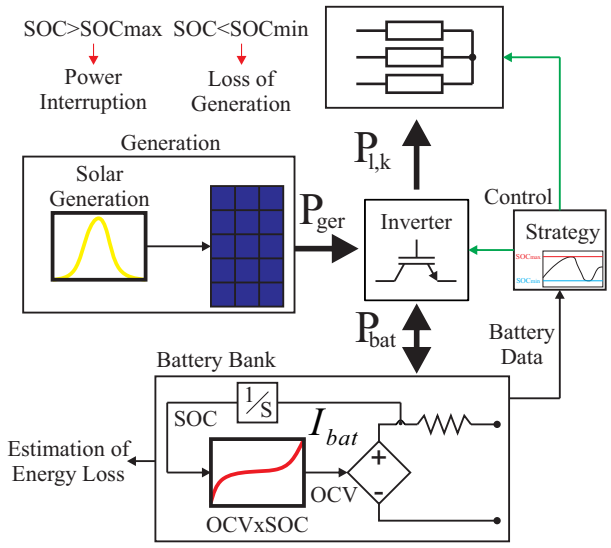

FIGURE 4. Display of the simplified version of the isolated power system considered for framework.

resource limitation assessment, and (iv) realistic timing behavior under computational load.

III. POWER FLOW AND ENERGY STORAGE STRATEGIES

In this study, an isolated power system is considered, and its main system simulated in the DSP. Moreover, these systems may suffer from intermittent generation due to atmospheric conditions, mainly photovoltaic generation due to its widespread use and sustainability [16]. To mitigate these issues, different generation systems may be implemented, or storage systems can be used, providing energy during moments of low generation and high demand [17]. A possible solution for the storage system is the use of BESS, which allows support during critical moments with low available generation [18]. Figure 4 shows the power flow of such a system.

The simulation is executed by the power flow in the system given by:

$$P_{bat} = P_{ger} - \sum_{n=1}^{n} P_{l,k}, \tag{1}$$

where P_{bat} is the power required by the battery bank, P_{ger} is the generated power and $P_{l,k}$ is the kth load power consumption, with a total of n loads.

The battery bank can be represented by various elements to illustrate its behavior. In an electrical model, the battery's voltage can involve multiple circuit components to capture specific characteristics, such as the open circuit voltage's dependence on the SOC, the series resistance, hysteresis effects during charging and discharging, and capacitive behavior [19]. However, in this model, only the open circuit voltage and series resistance are considered, where the SOC is estimated by the coulomb counting method given by:

$$SOC = \int_0^T \frac{i_{bat}(t)}{C}\, dt, \tag{2}$$

where T is the period of integration, t is the time, i_{bat} is the battery current and C is the battery capacity.

Furthermore, for the generation in the system, both irradiance and temperature are taken into account for the effects in P_{ger}, this can be described by:

$$P_{ger} = \eta_{mod}\ \eta_{sis}\ N_{mod} A_{mod}\ I_{rad}\ K_p\ \Delta T, \tag{3}$$

where η_{mod} and η_{sis} represent the photovoltaic module and system efficiency, respectively; N_{mod} is the number of modules; A_{mod} is the area of the modules; K_p is the temperature coefficient of power; I_{rad} is the irradiance; and ΔT is the ambient temperature variation relative to the standard test conditions. Both I_{rad} and ΔT are obtained from the broker through an Application Programming Interface (API), which allows the system to access irradiance and temperature variation data automatically for performance calculations.

Therefore, depending on the power generation P_{ger}, the energy availability tied to SOC, and the load demand $\sum_{n=1}^{n} P_{l,k}$, the system may face two extreme conditions: curtailment, when generation exceeds demand while SOC is at maximum, and total load shedding, when generation falls short of demand while SOC is at minimum [17].

IV. STRATEGY TO REDUCE THE LOAD SHEDDING

When considering isolated communities, one of the most important aspects with regard to the energy management is the loads that are present in the isolated system. Different types of load may impact the isolated system in different ways. Figure 5 shows some common types of load that may be encountered in isolated communities.

The standard situation in a three-phase system would be a balanced system, with the loads in each of the phases being equal to one another. However, this is rare to occur, since different loads are connected to the micro-grid and normally present different loads, resulting in an imbalanced system. Furthermore, some loads may be only passive and respond to voltage variations in the system, maintaining the consumed power. This may be achieved by power electronic converters and control structures. Moreover, in many situations, isolated communities require the use of inductive loads, such as water pumps and machines. These loads may have a great impact on the local grid, as they present a high initial current at start and may demand high power and energy. Furthermore, current loads, while requiring the same amount of current, may present reduced power [20].

Moreover, different types of load profiles may lead to varying levels of stress and energy usage during different hours of the day. For example, a load profile with a peak may present greater energy usage during the end of the day, a period without energy generation from a photovoltaic source, potentially leading to an energy shortage if the SOC

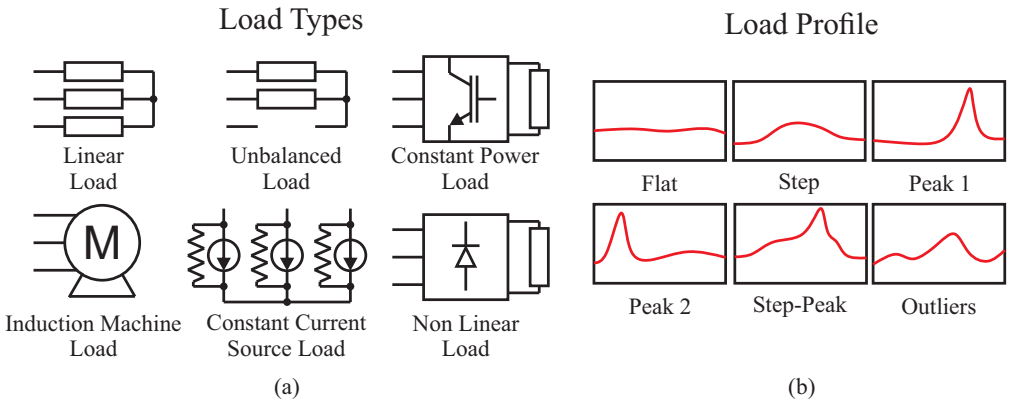

FIGURE 5. Display of (a) different load types regarding their operational behavior, and (b) different load profiler during their load behavior, during a day of use.

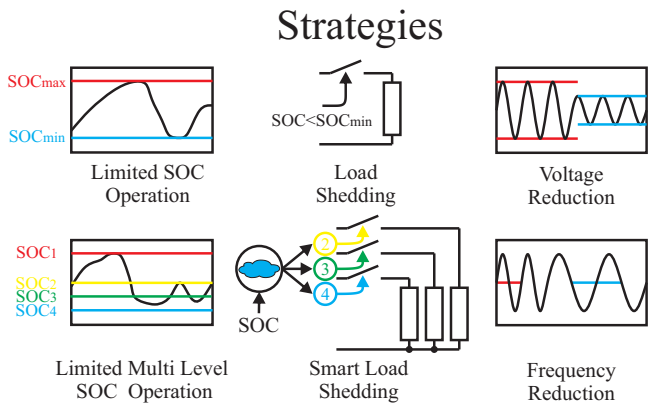

FIGURE 6. Display of different strategies for the SOC preservation.

is low. Additionally, the load profile may vary based on local installations and the time of year. Therefore, a fixed strategy may not be the most efficient in terms of energy usage [21].

Furthermore, intermediate SOC levels can be defined and used for load shedding, with each level representing a different priority of loads, aiming to conserve remaining energy. Therefore, less critical loads are disconnected to save energy for more critical and important loads. Moreover, there are different strategies to reduce load consumption in various ways. For example, voltage reduction can lead to decreased power consumption for non-constant power loads.

Considering strategies for standard operation, the charge controller of the batteries limits the SOC between a maximum value to avoid overcharge and a minimum value to prevent over-discharge, as shown in Figure 6. If these limits are not respected, the battery may suffer damage and reduced storage efficiency. Furthermore, while the standard practice is to use minimum and maximum SOC levels for battery protection, this may result in the load not having energy during certain operations of the day. In such a system, if there is a lack of energy and generation, all loads are disconnected from the grid, leading to total load shedding.

Other strategies can be employed to reduce the voltage delivered by the converter. This results in a decrease in power consumption for certain types of loads. However, constant power loads do not experience a reduction in consumption. This approach could offer a way to enhance system autonomy during critical periods of energy shortage [22]. Moreover, another strategy that can be used during critical stages of energy shortage is reducing the delivered frequency, which would primarily affect the power consumption of induction machines [23].

The system can adopt different load shedding strategies: either disconnect all loads at once or implement four priority levels, where each level reflects a different degree of importance for the loads. Priority 1 corresponds to the most critical load that should remain operational at all times, while lower priority loads can be deactivated as needed. The system is designed to selectively control the activation or deactivation of these loads.

Furthermore, four indices related to the quality and continuity of energy supply are considered: SAIFI (System Average Interruption Frequency Index), CAIFI (Customer Average Interruption Frequency Index), SAIDI (System Average Interruption Duration Index) and CAIDI (Customer Average Interruption Duration Index) [24]. Although typically applied to electric power distribution utility, this work extends these concepts to loads, treating each load as an individual consumer. These values represent potential interruptions that may occur when the battery cannot supply the required energy to the loads. Additionally, the energy curtailment resulting from the battery reaching full charge is estimated.

A. LOAD PRIORITY CLASSIFICATION

The system classifies loads into four priority levels based on their criticality to the power system operation:

- **Priority 1 (Critical):** Essential loads that must remain operational at all times (e.g., emergency lighting, communication systems)
- **Priority 2 (High):** Important loads with moderate interruption tolerance (e.g., refrigeration, water pumping)

- **Priority 3 (Medium):** Semi-critical loads that can tolerate longer interruptions (e.g., general lighting)
- **Priority 4 (Low):** Non-essential loads that can be disconnected first (e.g., recreational equipment)

B. SOC-BASED DISCONNECTION ALGORITHM

The hierarchical load control runs as a periodic decision task. At each decision instant the broker receives as inputs the current battery SOC, the on/off status of each priority load $load[i]$, and the last disconnection timestamps. Using the SOC thresholds $threshold_i$ (Priority 4: 25%, 3: 20%, 2: 15%, 1: 0%), and a reconnection margin of 5% plus a minimum OFF time of 1 hour, commands are issued to the local controller via MQTT. The decision logic operates as follows: the broker scans the priorities from 4 down to 1 (from lowest to highest). If SOC is less than or equal to the threshold of the current priority and the corresponding load is ON, the broker issues an OFF command and stores the current time t_{curr} as the last disconnection $timestamp[i]$. Otherwise, if SOC exceeds the threshold plus the 5% margin, the load is currently OFF, and at least one hour has elapsed since the last disconnection, the broker issues an ON command. The 1-hour minimum OFF time acts as a hysteresis mechanism that prevents rapid cycling of the loads and reduces equipment stress. This evaluation repeats every decision period as described in the Test Procedure below.

Figure 7(a) shows the flowchart corresponding to the implemented decision logic in the cloud-based platform, and Figure 7(b) shows the algorithm implemented on NODE-Red, in the broker interface. Besides, the assembled physical prototype (DSP, CAN transceiver, and ESP32) is presented in Figure 7(c).

Furthermore, Figure 7(b) shows the Node-RED flowchart of the implemented algorithm, organized into three main sections. Part (1) creates an HTTP GET endpoint at /upload, which provides a web interface that allows users to upload a CSV file. When the endpoint is accessed, the corresponding HTML page is displayed, and the HTTP node returns it to the browser. Part (2) defines an HTTP POST endpoint at $/upload_{data}$, responsible for processing the uploaded CSV file. It retrieves the file from msg.req.files, parses it using a CSV parser, and extracts the relevant variables. These variables are those used in our system to simulate the loads and climate conditions. Finally, part (3) manages communication with an ESP device through an MQTT topic. It listens for incoming messages, which can be either data requests or responses. When a request is received, it sends the required data back to the device, while logging nodes record and store all responses in the database.

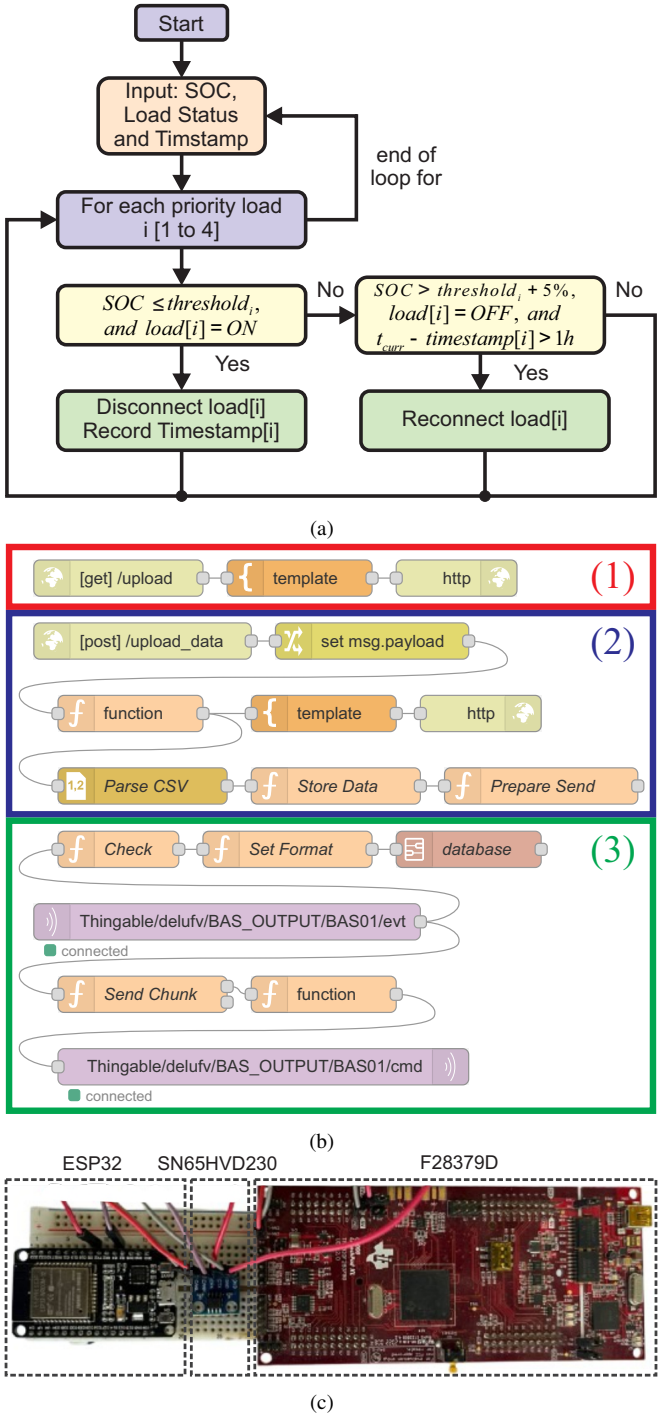

FIGURE 7. (a) Flowchart of the hierarchical load shedding strategy implemented in the broker. (b) Node-RED flowchart of the implemented algorithm. (c) Physical prototype: DSP, CAN transceiver and ESP32.

V. CASE STUDY

For the implementation of the system, a DSP from Texas Instruments, model F28379D, is responsible for the BESS local controller, including current and power loop control, as detailed in [25] and shown in Figure 3, where the simulation

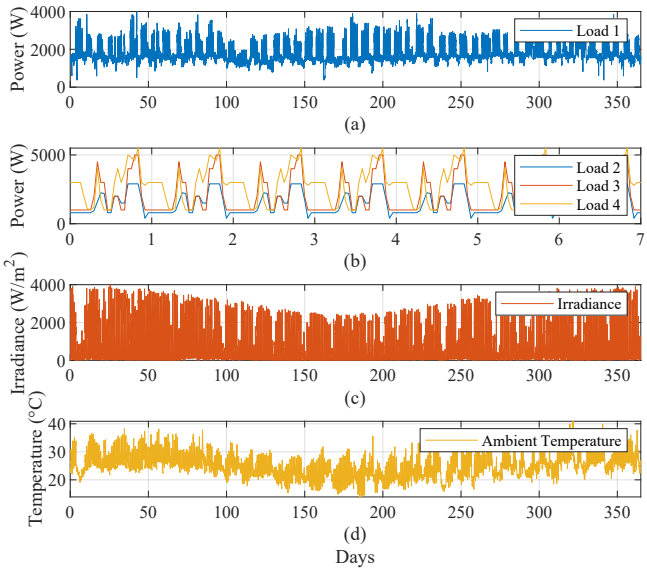

FIGURE 8. Display of the data used for the simulation for the profile for (a) Load 1, (b) Load 2, 3 and 4, (c) Irradiance and (d) temperature.

is implemented. The operation and control references are sent by *thingable!* according to the system necessities and forecast conditions.

The key information for the test is presented in Figure 8. Figure 8(a) illustrates the load profile of a single load over an entire year [26], while Figure 8(b) displays the profile for loads 2, 3, and 4 over the course of one week [27], with this profile being repeated throughout the rest of the year. Figures 8(c) and (d) depict the local irradiance and temperature, respectively [28].

The selected module for the system is the 72HC-BDVP from Jinko [29]. Using this module, a total of 84 units are required to meet the load demands presented in Figures 8(a)-(b), taking into account the irradiance shown in Figure 8(c). Additionally, the isolated power system is designed to provide 3 days of autonomy, utilizing lithium iron phosphate cells from WEG [30], with a capacity of 280 Ah, requiring 33 battery packs connected in parallel.

Furthermore, two different strategies for testing the system communication and operation are considered. The traditional strategy consists of total load shedding, disconnecting all loads simultaneously when the battery reaches minimum SOC values of 0%. The Shedding strategy disconnects loads 1, 2, 3 and 4 in order of importance at SOC values of 0%, 15%, 20% and 25%, respectively. Moreover, when a load is disconnected, it can only be reconnected after a delay of 1 hour.

The resulting system comprises a 50 kW photovoltaic inverter, and an average monthly energy delivery of 6 MWh. The system also includes a connected BESS with the same power, and a capacity of 9.2 kAh, at a discharge rate of 0.5 C [30].

Regarding the loads, ordered from highest to lowest priority, Load 1 presents a peak power demand of 3.8 kW and an average power of 1.8 kW. Load 2 has a peak demand of 2.9 kW, with an average of 1.5 kW. Load 3 reaches a peak power of 5.0 kW and an average demand of 1.9 kW, while Load 4 exhibits a peak power of 5.5 kW with an average power consumption of 2.3 kW.

The broker communicates every 15 minutes, synchronized with the DSP simulation step for demand/generation aggregation, while the power-flow runs at 1 s. Commands are transmitted to the ESP32 with MQTT QoS 2; acknowledgments and execution times are logged. For each event it is record: timestamp, SOC, load index, action (ON/OFF), and round-trip latency. The 1-hour hysteresis window is enforced with the server-side timestamps to avoid oscillations. Over the one-year dataset, we compute: (i) reliability indices per load (SAIFI, SAIDI, CAIDI, CAIFI), (ii) average SOC, and (iii) curtailed energy and energy not served. These metrics are the basis of the comparisons presented in the Results section.

VI. RESULTS AND DISCUSSION

The effectiveness of the load-shedding strategies in enhancing battery lifespan and grid resilience was evaluated through a framework using the CIL approach.

Figure 9 compares the SOC of the BESS under the two strategies. The traditional strategy, representing a total load shedding upon reaching 0% SOC, proves impractical for isolated power systems. This abrupt disconnection can trigger power outages in critical areas, undermining system reliability. A more nuanced approach is required, one that prioritizes essential loads and optimizes battery usage. Figures 9(c) and 9(d) provide a closer examination of the SOC behavior when it reaches its minimum for both strategies.

The Shedding strategy addresses these concerns by disconnecting loads in order of importance at predefined SOC levels. This approach ensures continuous power to critical loads, enhancing system quality, minimizing strain on the battery bank, and extending operational time during periods of limited power availability. Figure 9(b) illustrates the SOC of the BESS under the shedding strategy. Notably, the system never reaches a 0% SOC, operating within a range that promotes long-term battery health and ensures uninterrupted power to essential loads. This proactive strategy bolsters the system ability to manage energy storage effectively, especially in critical situations common to isolated energy systems.

Figure 10 shows the power flow within the BESS. The input power to the battery system is calculated as the generation minus the loads, minus the power drawn from the battery. This visualization reveals the dynamic interplay between energy generation, consumption, and storage. Notably, Strategies 1 and 2 exhibit distinct power flow characteristics due to load interruptions based on SOC, as evident in Figures 10(a) and 10(b). To understand the power flow dynamics under the traditional strategy, Figure

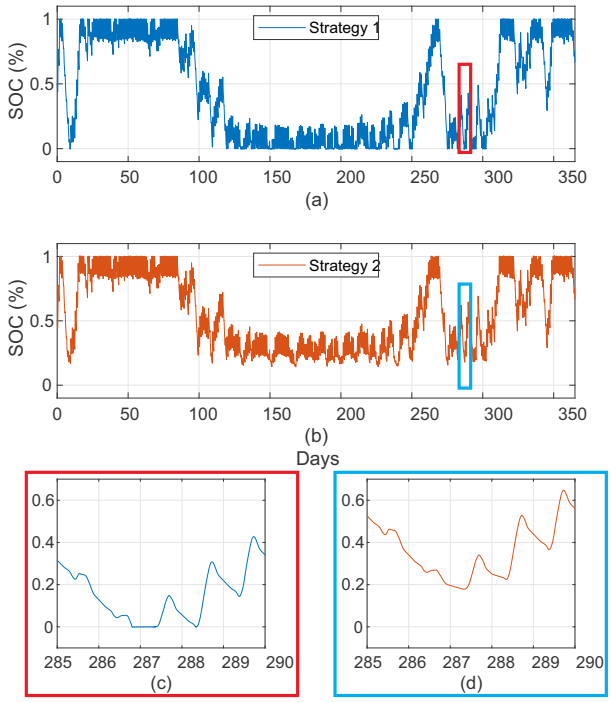

FIGURE 9. Display of the SOC for the (a) Traditional strategy, (b) Shedding strategy. The zoomed regions are color-coded to indicate data for (c) the Traditional strategy and (d) the Shedding strategy.

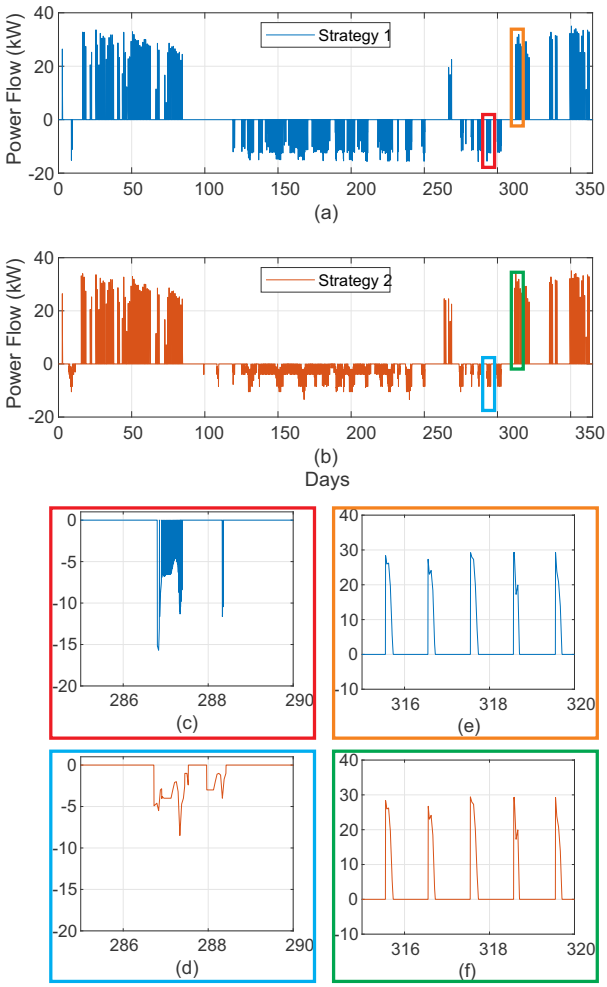

FIGURE 10. Display of the non delivered BESS Power Flow for the (a) Traditional strategy, (b) Shedding strategy. The zoomed regions are color-coded to indicate data for (c) the Traditional strategy and (d) the shedding strategy, when the battery cannot feed the system, and then it can not receive power (c) the Traditional strategy and (d) the shedding strategy.

10(c) focuses on a period of higher power output from the battery, while Figure 10(d) focuses on a period of higher power input to the battery. Comparing these figures to Figures 10(e) and 10(f), which illustrate higher output and input for the shedding strategy, reveals a smoother power flow profile with fewer higher outputs for the shedding strategy, because of the hierarchical load shedding.

Figures 11 and 12 illustrate the load profiles under the traditional strategy and the shedding strategy, respectively. Under the traditional strategy, all loads experience a complete shutdown, as depicted in Figure 11. Figures 11(e) through 11(h) illustrate the abrupt nature of load disconnections under the traditional strategy, highlighting the potential for disruptions to essential services. In contrast, the shedding strategy is more sophisticated control ensures the uninterrupted operation of the most critical load, Load 1, as shown in Figure 12(a). This highlights the strategy effectiveness in maintaining essential services even during periods of energy scarcity. Figures 12(e) through 12(h) show that even though loads 2, 3, and 4 experience periods of disconnection under the shedding strategy, these disconnections are not as abrupt or complete as those seen under the traditional strategy.

Table 2 presents an overview of the resilience, showing the impact of the two different control strategies on system performance. The metrics include average SOC, the number of system interruptions (intr.) per load (SAIFI), the total interruption time for each load (SAIDI), the average duration of each load interruption (CAIDI), and the average frequency of sustained interruptions per customer (CAIFI). Each load is treated as an individual customer for calculating CAIFI, therefore it's the same value as SAIFI.

Traditional strategy, which represents total load shedding upon reaching a 0% SOC, results in an average SOC of 43.64% and 534 energy outages across all loads. This abrupt disconnection of all loads simultaneously when the battery is depleted can lead to system instability and negatively impact overall system reliability. The frequent and short interruptions experienced by all loads under the traditional strategy can disrupt essential services.

The shedding strategy involves disconnecting loads based on a hierarchy of importance at predefined SOC levels. This strategy yields a higher average SOC of 54.66%. By implementing this selective shedding approach, the system can stabilize more effectively, maintain satisfactory battery charge levels, and extend operational time during periods of limited power availability. Notably, Load 1,

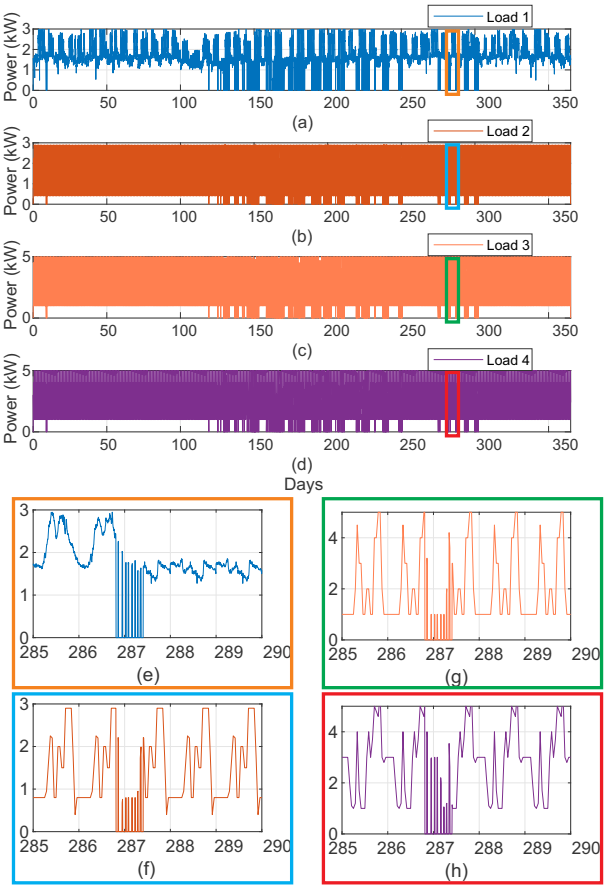

FIGURE 11. Load profile for the traditional strategy (a) Load 1, (b) Load 2, (c) Load 3, (d) Load 4. The zoomed regions are color-coded to indicate data for (e) Load 1, (f) Load 2, (g) Load 3, (h) Load 4.

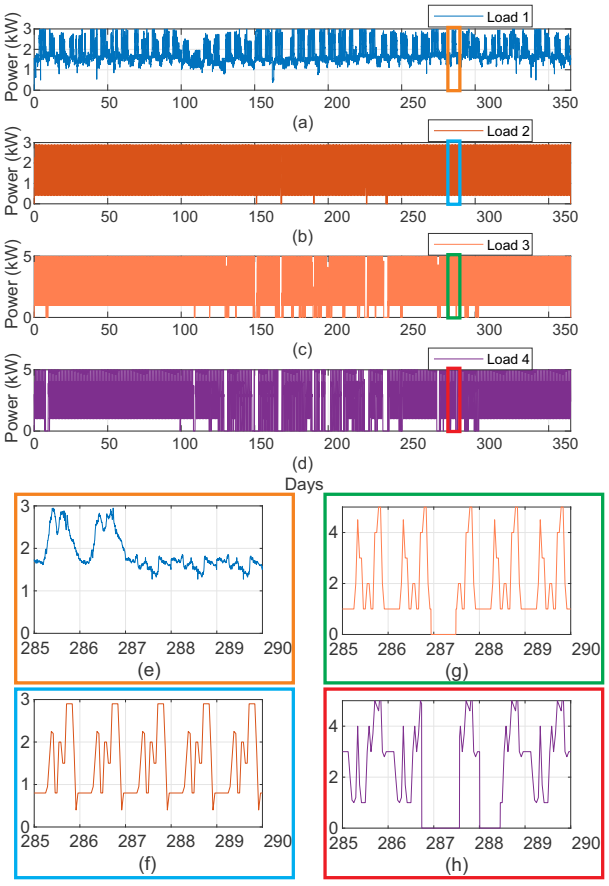

FIGURE 12. Load profile for the shedding strategy (a) Load 1, (b) Load 2, (c) Load 3, (d) Load 4. The zoomed regions are color-coded to indicate data for (e) Load 1, (f) Load 2, (g) Load 3, (h) Load 4.

the most critical load, experiences no interruptions under the shedding strategy, ensuring its consistent operation and highlighting the effectiveness of this strategy in maintaining essential services, even during periods of energy scarcity. Although Load 4, the least critical load, experiences more frequent, longer-duration disconnections under the shedding strategy compared to the traditional strategy, this is a necessary trade-off to prioritize the continuous operation of higher-priority loads.

TABLE 2. Grid Resilience Metrics

Metric	Traditional strategy	Shedding strategy
Average SOC (%)	43.64	54.66
SAIFI (intr./year)	Load 1: 534 Load 2: 534 Load 3: 534 Load 4: 534	Load 1: 0 Load 2: 8 Load 3: 56 Load 4: 114
SAIDI (hours/year)	Load 1: 701.52 Load 2: 701.52 Load 3: 701.52 Load 4: 701.52	Load 1: 0 Load 2: 52.8 Load 3: 724.8 Load 4: 1536
CAIDI (hours/intr.)	Load 1: 1.32 Load 2: 1.32 Load 3: 1.32 Load 4: 1.32	Load 1: N/A Load 2: 6.67 Load 3: 12.89 Load 4: 16.00

Based on the results obtained with the traditional and hierarchical shedding strategies, additional measures can be considered to further reduce the SAIFI. One possible approach is increasing the number of photovoltaic panels and, consequently, the overall power generation. Since most interruptions occur during the winter period, as shown in Figures 11 and 12, increasing the storage capacity alone would not be sufficient, as the available generated power during this period is not enough to significantly impact the SAIFI values.

These results show that the proposed CIL structure, which integrates a hierarchical load shedding strategy with IoT-based monitoring and control, allows for a framework of the system communication in the IoT network.

VII. CONCLUSION

This work proposed a Cloud-in-the-Loop framework that integrates IoT communication, cloud-based monitoring, and hardware-in-the-loop simulation to support the development and validation of advanced control strategies. The case study with a Battery Energy Storage System in an isolated

network served as an illustrative example, demonstrating the framework's ability to assess long-term operation under realistic conditions. More importantly, the proposed approach is not limited to this specific application: it can be extended to a wide range of energy and automation systems where IoT-based monitoring and control are required. By keeping the cloud functionalities unchanged and replacing only the physical hardware, the framework establishes an intermediate validation stage that reduces or eliminates implementation issues. This contribution highlights the framework's role as a practical and scalable tool to bridge the gap between conceptual design and real-world deployment, ensuring higher reliability and robustness of IoT-enabled solutions.

ACKNOWLEDGMENT

This work was supported in part by Conselho Nacional de Desenvolvimento Científico e Tecnológico (CNPq) (Projects: 307172/2022-8; 407926/2023-2; 443170/2023-1), Coordenação de Aperfeiçoamento de Pessoal de Nível Superior (CAPES), Fundação de Amparo à Pesquisa de Minas Gerais (FAPEMIG) (Projects : RED-00216-23; APQ-03164-24). The authors would also like to thank the CONCERT for the support and for providing access to the *thingable!* platform.

AUTHOR'S CONTRIBUTIONS

D.GONÇALVES: Formal Analysis, Methodology, Software, Validation, Writing – Original Draft, Writing – Review & Editing. **I.O.FURTADO:** Conceptualization, Methodology, Software, Validation, Writing – Original Draft, Writing – Review & Editing. **A.F.CUPERTINO:** Conceptualization, Funding Acquisition, Project Administration, Resources, Supervision, Writing – Review & Editing. **H.A.PEREIRA:** Conceptualization, Funding Acquisition, Methodology, Project Administration, Resources, Supervision, Writing – Original Draft, Writing – Review & Editing. **R.TEODORESCU:** Conceptualization, Investigation, Methodology, Project Administration, Supervision, Validation, Writing – Review & Editing.

PLAGIARISM POLICY

This article was submitted to the similarity system provided by Crossref and powered by iThenticate – Similarity Check.

DATA AVAILABILITY

The data used in this research is available in the body of the document.

REFERENCES

[1] A. von Jouanne, E. Agamloh, A. Yokochi, "Power Hardware-in-the-Loop (PHIL): A Review to Advance Smart Inverter-Based Grid-Edge Solutions", *Energies*, vol. 16, no. 2, 2023, doi:10.3390/en16020916.

[2] H. Magnago, H. Figueira, O. Gagrica, D. Majstorovic, "HIL-based certification for converter controllers: Advantages, challenges and outlooks (Invited Paper)", *in 2021 21st International Symposium on Power Electronics (Ee)*, pp. 1–6, 2021, doi:10.1109/Ee53374.2021.9628196.

[3] J. Saele, I. O'Bryan, "Realization of Real-Time Simulation of Power Electronics Systems in Applications - A Review of Requirements and Methods", *in 2024 IEEE 15th International Symposium on Power Electronics for Distributed Generation Systems (PEDG)*, pp. 1–6, 2024, doi:10.1109/PEDG61800.2024.10667355.

[4] C. S. B. Clausen, B. N. Jørgensen, Z. G. Ma, "A scoping review of In-the-loop paradigms in the energy sector focusing on software-in-the-loop", *Energy Informatics*, vol. 7, no. 1, p. 12, 2024, doi:10.1186/s42162-024-00312-8.

[5] L. C. Hidalgo Monsivais, Y. León Ruiz, J. C. Hernández Ramírez, N. Visairo-Cruz, J. Segundo-Ramírez, E. Barocio, "Controller Hardware-in-the-Loop Validation of a DSP-Controlled Grid-Tied Inverter Using Impedance and Time-Domain Approaches", *Electricity*, vol. 6, no. 3, 2025, doi:10.3390/electricity6030052.

[6] P. Lamo, A. de Castro, A. Sanchez, G. A. Ruiz, F. J. Azcondo, A. Pigazo, "Hardware-in-the-Loop and Digital Control Techniques Applied to Single-Phase PFC Converters", *Electronics*, vol. 10, no. 13, 2021, doi:10.3390/electronics10131563.

[7] L. F. R. Menegazzo, A. L. N. Severo, L. B. Piton, C. M. de Freitas, R. J. F. Bortolini, L. V. Bellinaso, L. Michels, F. de Morais Carnielutti, "Unified Platform for Automated Tests of Inverter-Based Resources with Hardware-in-the-loop", *Eletrônica de Potência*, vol. 29, p. e202443, Oct. 2024, doi:10.18618/REP.e202443.

[8] A. von Jouanne, E. Agamloh, A. Yokochi, "Power Hardware-in-the-Loop (PHIL): A Review to Advance Smart Inverter-Based Grid-Edge Solutions", *Energies*, vol. 16, no. 2, 2023, doi:10.3390/en16020916.

[9] F. Mihalič, M. Truntič, A. Hren, "Hardware-in-the-Loop Simulations: A Historical Overview of Engineering Challenges", *Electronics*, vol. 11, no. 15, 2022, doi:10.3390/electronics11152462.

[10] D. Gebbran, A. Barragán-Moreno, P. I. Gómez, R. K. Subroto, M. M. Mardani, M. López, J. Quiroz, T. Dragičević, "Cloud and Edge Computing for Smart Management of Power Electronic Converter Fleets: A Key Connective Fabric to Enable the Green Transition", *IEEE Industrial Electronics Magazine*, vol. 17, no. 2, pp. 6–19, 2023, doi:10.1109/MIE.2022.3211125.

[11] S. H. Jeon, J. Lee, J. K. Choi, "Energy Outage-Aware Power Distribution Scheme for Off-Grid Base Station Operation", *IEEE Communications Letters*, vol. 21, no. 6, pp. 1401–1404, 2017, doi:10.1109/LCOMM.2017.2676108.

[12] R. d. S. Ferraz, S. G. M. Oliveira, H. Tertuliano dos S. Filho, C. Bastos da Silva, "Design and Autonomy Evaluation of a Power Supply for Long Range IoT Devices Using Magnetic Field Harvested Energy from High Current", *Eletrônica de Potência*, vol. 29, p. e202429, Sep 2024, doi:10.18618/REP.e202429.

[13] D. Tan, "Power Electronics: Historical Notes, Recent Advances and Contemporary Challenges", *Eletrônica de Potência*, vol. 25, no. 4, pp. 386–394, Dec 2020, doi:10.18618/REP.2020.4.00701.

[14] X. Hu, Y. Che, X. Lin, S. Onori, "Battery Health Prediction Using Fusion-Based Feature Selection and Machine Learning", *IEEE Transactions on Transportation Electrification*, vol. 7, no. 2, pp. 382–398, 2021, doi:10.1109/TTE.2020.3017090.

[15] CONCERT Technologies, "thingable! IoT Platform", https://www.thingable.com.br, access on May 30, 2023.

[16] E. Gonschorowski, R. Cardoso, E. L. Carvalho, C. M. d. O. Stein, E. G. Carati, G. W. Denardin, J. P. Costa, "Adaptive Frequency-Based Power Management for Off-Grid Hybrid Photovoltaic Converters", *Eletrônica de Potência*, vol. 29, p. 22, 2024, doi:10.18618/REP.e202440.

[17] V. B. Costa, R. S. Capaz, B. D. Bonatto, "Small steps towards energy poverty mitigation: Life cycle assessment and economic feasibility analysis of a photovoltaic and battery system in a Brazilian indigenous community", *Renewable and Sustainable Energy Reviews*, vol. 180, p. 113266, 2023, doi:10.1016/j.rser.2023.113266.

[18] S. Jain, S. Dhara, V. Agarwal, "A Voltage-Zone Based Power Management Scheme With Seamless Power Transfer Between PV-Battery for OFF-Grid Stand-Alone System", *IEEE Transactions on Industry Applications*, vol. 57, no. 1, pp. 754–763, 2021, doi:10.1109/TIA.2020.3031265.

[19] G. Plett, *Battery Management Systems, Volume I: Battery Modeling*, Artech House power engineering series, Artech House, 2015.

[20] E. Liu, Y. Han, A. S. Zalhaf, P. Yang, C. Wang, "Performance evaluation of isolated three-phase voltage source inverter with LC

filter adopting different MPC methods under various types of load", *Control Engineering Practice*, vol. 135, p. 105520, 2023, doi:10.1016/j.conengprac.2023.105520.
[21] L. Lorenzoni, P. Cherubini, D. Fioriti, D. Poli, A. Micangeli, R. Giglioli, "Classification and modeling of load profiles of isolated mini-grids in developing countries: A data-driven approach", *Energy for Sustainable Development*, vol. 59, pp. 208–225, 2020, doi:10.1016/j.esd.2020.10.001.
[22] R. Faranda, H. Hafezi, "Reassessment of voltage variation for load power and energy demand management", *International Journal of Electrical Power & Energy Systems*, vol. 106, pp. 320–326, 2019, doi:10.1016/j.ijepes.2018.10.012.
[23] M. Farrokhabadi, C. A. Cañizares, K. Bhattacharya, "Frequency Control in Isolated/Islanded Microgrids Through Voltage Regulation", *IEEE Transactions on Smart Grid*, vol. 8, no. 3, pp. 1185–1194, 2017, doi:10.1109/TSG.2015.2479576.
[24] ANEEL, "Procedimentos de Distribuição de Energia Elétrica no Sistema Elétrico Nacional (PRODIST) - Módulo 8: Qualidade da Energia Elétrica", , 2023.
[25] L. S. Xavier, A. F. Cupertino, H. A. Pereira, V. F. Mendes, "Power Control Strategy for Grid-Connected Inverters in Stationary Reference Frame", *Eletrônica de Potência*, vol. 27, no. 2, pp. 129–138, 2022, doi:10.18618/REP.2022.2.0048.
[26] R. Cassio de Barros, W. Caires Silva Amorim, W. do Couto Boaventura, A. Fagner Cupertino, V. Flores Mendes, H. Augusto Pereira, "Methodology for BESS Design Assisted by Choice Matrix Approach", *Eletrônica de Potência*, vol. 29, p. e202412, 2024, doi:10.18618/REP.2005.1.019027.
[27] K. S. Gyamfi, E. Gaura, J. Brusey, A. B. Trindade, N. Verba, "Understanding Household Fuel Choice Behaviour in the Amazonas State, Brazil: Effects of Validation and Feature Selection", *Energies*, vol. 13, no. 15, 2020, doi:10.3390/en13153857.
[28] I. N. de Meteorologia, "Dados Históricos Anuais", Accessed on September 09, 2024, 2023, URL: https://portal.inmet.gov.br/dadoshistoricos.
[29] J. Solar, "Tiger Pro 72HC-BDVP 535-555 Watt", Accessed on September 09, 2024, 2020, URL: https://jinkosolarcdn.shwebspace.com/uploads/JKM535-555M-72HL4-BDVP-F6%20EN.pdf.
[30] WEG, "Sistema de Armazenamento de Energia em Baterias", Accessed on September 09, 2024, 2021, URL: https://static.weg.net/medias/downloadcenter/hc7/h38/WEG-ESSW-sistema-de-armazenamento-de-energia-50100243-pt.pdf.

BIOGRAPHIES

Diuary Gonçalves received the B.S. degree in electrical engineering from the Universidade Federal de Viçosa, Viçosa, Brazil, in 2022, and the M.S. degree in electrical engineering from the Centro Federal de Educação Tecnológica of Minas Gerais, Belo Horizonte, Brazil, in 2023. Currently doing his Ph.D. degree in electrical engineering from the Federal Center for Technological Education of Minas Gerais, Belo Horizonte, Brazil. He is currently a Federal Institute Professor at the Department of Electrical Engineering, Centro Federal de Educação Tecnológica Celso Suckow da Fonseca - Nova Friburgo, Rio de Janeiro, Brazil. His main research interests include battery energy storage systems, battery state of health and charge estimation, and photovoltaic inverter control and modelling.

Ives de Oliveira Furtado is a Master's candidate in Electrical Engineering at the Centro Federal de Educação Tecnológica de Minas Gerais (CEFET-MG). His research focuses on photovoltaic module characterization and performance monitoring systems. He is a member of the research group GESEP (Gerência de Especialistas em Sistemas Elétricos de Potência) at the Universidade Federal de Viçosa. His main research interests include photovoltaic systems, embedded systems, IoT applications for renewable energy, and signal processing for power electronics.

Allan Fagner Cupertino received the Bachelor's degree in Electrical Engineering from the Federal University of Viçosa in 2013, and the Master's and Doctoral degrees in Electrical Engineering from the Federal University of Minas Gerais in 2015 and 2019, respectively. Was a visiting Ph.D. student at the Department of Energy Technology at Aalborg University from 2018 to 2019. From 2014 to 2022, was an Assistant Professor at the Federal Center for Technological Education of Minas Gerais. Since 2023, has been with the Department of Electrical Energy at the Federal University of Juiz de Fora. His main research interests include renewable energy conversion systems, smart battery energy storage systems, cascaded multilevel converters, and reliability. Prof. Cupertino was awarded the President Bernardes Silver Medal in 2013, the SOBRAEP Doctoral Thesis Award in 2020, and the IAS CMD Doctoral Thesis Contest in 2021. He is a member of the Brazilian Power Electronics Society and the Brazilian Society of Automatics.

Heverton Augusto Pereira obtained the Bachelor's degree in Electrical Engineering from the Federal University of Viçosa, Brazil, in 2007, the Master's degree from the State University of Campinas in 2009, and the Doctoral degree from the Federal University of Minas Gerais in 2015, all in the field of Electrical Engineering. Was a visiting researcher at the Department of Energy Technology at Aalborg University, Denmark, in 2014. Has been working as an Associate Professor in the Department of Electrical Engineering at UFV since 2009. His main research interests include grid-connected converters for solar energy systems and energy storage systems.

Remus Teodorescu received a Dipl. Ing. degree in Electrical Engineering from the Polytechnical University of Bucharest, Bucharest, Romania, in 1989, and a Ph.D. degree in Power Electronics from the University of Galati, Galati, Romania, in 1994. Since 1998, he has been working with the Power Electronics Section, Department of Energy Technology, Aalborg University, Aalborg, Denmark, where he is currently a Professor. He is the Founder and Coordinator of the Green Power Laboratory, Aalborg University, focusing on the development and testing of grid converters for renewable energy systems. He is the Coordinator of the Vestas Power Program involving ten Ph.D. students, two postdoctoral researchers, and Guest Professors in the areas of Power Electronics, Power Systems, and Energy Storage. His areas of interest are the design and control of power converters used in photovoltaics and wind-power systems, grid integration with wind power, medium-voltage converters, and high-voltage direct current/flexible ac transmission system energy storage. He is a Past Associate Editor of the IEEE Transactions on Power Electronics and Chair of the IEEE Danish joint IES/PELS/IAS chapter.